hsa-miR-9-3p and hsa-miR-9-5p as Post-Transcriptional Modulators of DNA Topoisomerase IIα in Human Leukemia K562 Cells with Acquired Resistance to Etoposide

Evan E. Kania, Jessika Carvajal-Moreno, Victor A. Hernandez, Anthony English, Jonathan L. Papa, Nicholas Shkolnikov, Hatice Guclin Ozer, Ayse Selen Yilmaz, Jack C. Yalowich, and Terry S. Elton

Division of Pharmaceutics and Pharmacology, College of Pharmacy (EEK, JCM, VAH, AE, JP, NS, JCY, TSE); Department of Biomedical Informatics, College of Medicine (HGO, ASY), The Ohio State University, Columbus, Ohio

Running title: hsa-miR-9-3p and hsa-miR-9-5p function in drug resistance

Corresponding authors: Jack C. Yalowich, Division of Pharmaceutics and Pharmacology, College of Pharmacy, The Ohio State University, 500 West 12th Avenue, Columbus, Ohio, 43210; Tel. 614-688-5980, Fax: 614-292-5369; or: Terry S. Elton, Division of Pharmaceutics and Pharmacology, College of Pharmacy, The Ohio State University, 500 West 12th Avenue, Columbus, Ohio, 43210; Tel. 614-292-1400, Fax: 614-292-5369. E-mail: yalowich.1@osu.edu (J.C. Yalowich); elton.8@osu.edu (T.S. Elton)

Number of Text Pages: 44

Number of Table(s): 0

Number of Figures: 5

Number of Supplemental Figure(s): 0

Number of References: 79

Number of Words in Abstract: 250

Number of Words in Significance Statement: 58

Number of Words in Introduction: 748

Number of Words in Discussion: 1500

Abbreviations: ABCB1, multidrug resistance protein 1/P-glycoprotein; ADR, Adriamycin; AML, acute myeloid leukemia; DMEM, Dulbecco's modified Eagle's medium; DMSO, dimethylsulfoxide; EOC, epithelial ovarian carcinoma; FBS, fetal bovine serum; GAPDH, glyceraldehyde 3-phosphate dehydrogenase; K562, human leukemia cell line; K/VP.5, etoposide (VP-16)-resistant human K562 leukemia cell line; kDa, kilodalton; miRNA, microRNA; miRISC, miRNA-RISC complex; MREs, miRNA recognition elements; PBS, phosphate-buffered saline; PCR, polymerase chain reaction; pre-miRNA, precursor miRNA; pri-miRNAs, primary miRNA transcripts; PVDF, polyvinylidene difluoride; qPCR, quantitative PCR; RISC, RNA-induced silencing complex; RUNX, runt-related; SHH, Sonic Hedgehog; TBP, TATA-binding protein; TOP2α, DNA topoisomerase IIα protein; TOP2α /170, TOP2α 170 kDa; TOP2α /90, TOP2α 90 kDa; UTR, untranslated region

Abstract

DNA topoisomerase IIα (TOP2α/170) is an important target for anticancer agents whose efficacy is often attenuated by chemoresistance. Our laboratory has characterized acquired resistance to etoposide in human leukemia K562 cells. The clonal resistant subline, K/VP.5, contains reduced TOP2α/170 mRNA and protein levels compared to parental K562 cells. The aim of this study was to determine whether miRNA-mediated mechanisms play a role in drug resistance via decreased expression of TOP2α/170. miRNA-sequencing revealed that human miR-9-3p and miR-9-5p were among the top six of those overexpressed in K/VP.5 compared to K562 cells; validation by qPCR demonstrated overexpression of both miRNAs. miRNA recognition elements (MREs) for both miRNAs are present in the 3′-UTR of TOP2α/170. Transfecting K562 cells with a reporter plasmid harboring the TOP2α/170 3′-UTR together with either miR-9-3p or miR-9-5p mimics resulted in a statistically significant decrease in luciferase expression. Mutating the miR-9-3p or miR-9-5p MREs prevented this decrease, demonstrating direct interaction between these miRNAs and TOP2α/170 mRNA. Transfection of K562 cells with miR-9-3p or miR-9-5p mimics led to decreased TOP2α/170 protein levels without a change in TOP2α/170 mRNA, and resulted in attenuated etoposide-induced DNA damage (gain-of-miRNA-inhibitory function). Conversely, transfection of miR-9-3p or miR-9-5p inhibitors in K/VP.5 cells (overexpressed miR-9 and low TOP2α/170) led to increased TOP2α/170 protein expression without a change in TOP2α/170 mRNA levels, and resulted in enhancement of etoposide-induced DNA damage (loss-of-miRNA-inhibitory function). Taken together, these results strongly suggest that these miRNAs play a role in and are potential targets for circumvention of acquired resistance to etoposide.

3

Significance Statement

Results presented here indicate that miR-9-3p and miR-9-5p decrease TOP2α/170 expression levels in acquired resistance to etoposide. These findings contribute new information about and potential strategies for circumvention of drug resistance; by modulation of miRNA levels. Furthermore, increased expression of miR-9-3p and miR-9-5p in chemoresistant cancer cells may support their validation as biomarkers of responsiveness to TOP2-targeted therapy.

Introduction

DNA topoisomerase IIα (170 kDa, TOP2α/170) induces covalent complexes with DNA and produces transient double-strand DNA breaks crucial for processes such as replication and chromosomal dysjunction at mitosis (Deweese and Osheroff, 2009). The TOP2α/170 enzyme exists as a homodimer. Each monomer utilizes a tyrosine active site as a nucleophile to begin a reversible transesterification reaction with 5′-nucleobase scissile sites on the phosphate backbones of the top or bottom strands of DNA (Deweese and Osheroff, 2009). This cleavage and subsequent rapid religation of DNA allows for the relaxation/separation of DNA entanglements (Vos et al., 2011; Chen et al., 2013; Pendleton et al., 2014; Ashour et al., 2015). TOP2α/170 has been utilized as an important target in cancer therapy (Larsen et al., 2003; Deweese and Osheroff, 2009; Nitiss, 2009; Pommier et al., 2010). Type IIA topoisomerase interfacial inhibitors, such as etoposide, stabilize the otherwise short-lived enzyme-DNA complexes by insertion within the four base pair scissile break sites generated by TOP2α/170 (Laponogov et al., 2010; Pommier et al., 2010) thereby inhibiting religation. Programmed cell death can ensue due to an aggregation of double-strand DNA breaks (Pommier et al., 2010).

Acquired resistance to TOP2α/170-targeted agents (e.g., etoposide, mitoxantrone, amsacrine, doxorubicin and analogs) is important clinically in the treatment of a variety of malignancies (Chen and Liu, 1994; Vassetzky et al., 1995; Pilati et al., 2012; Ganapathi and Ganapathi, 2013). While mutant forms of TOP2α have been reported in acquired resistance (Zwelling et al., 1989; Bugg et al., 1991; Hinds et al., 1991; Kubo et al., 1996), most evidence from selected cell lines (Ritke and Yalowich, 1993; Ritke et al, 1994; Mirski et al., 1993, 2000; Harker et al., 1995; Mirski and Cole, 1995; Wessel et al., 1997; Yu et al., 1997; Burgess et al., 2008) and patient samples (Ganapathi and Ganapathi, 2013) suggests that decreased levels of TOP2α is a major determinant of drug resistance. Our laboratory has previously demonstrated that

a cloned K562 cell line (designated K/VP.5 cells) with acquired resistance (~25-fold) to etoposide, expresses less TOP2α/170 protein compared to the parental K562 cells with no change in drug accumulation and no overexpression of ABCB1 (multidrug resistance protein 1/P-glycoprotein) (Ritke and Yalowich, 1993; Ritke et al, 1994). In addition, K/VP.5 cells overexpressed a novel TOP2α 90 kDa isoform (i.e., TOP2α/90), the translation product of TOP2α mRNA that retains a processed intron 19 (Kanagasabai et al., 2017; Kanagasabai et al., 2018). Importantly, the TOP2α/90 isoform heterodimerizes with the TOP2α/170 isoform resulting in a dominant-negative effect with respect to etoposide-induced covalent TOP2α-DNA complexes, DNA damage, and cytotoxicity (Kanagasabai et al., 2018). Together, literature indicates that acquired resistance to TOP2α-targeted agents can result from multiple mechanisms involving dysregulation of TOP2α.

MicroRNA (miRNA)-mediated post-transcriptional gene silencing is an established mechanism of genetic regulation (Bartel, 2009). Typically, mature non-coding miRNAs (21-25 nucleotides) are embedded in primary miRNA transcripts (pri-miRNAs) as imperfectly based-paired stem-loops (Ha and Kim, 2014). In the nucleus, pri-miRNA is further processed to a hairpin structured precursor miRNA (pre-miRNA) of ~60-70 nucleotides. Subsequently, in the cytoplasm, the terminal loop is removed and the resulting miRNA duplexes of ~22 nucleotides are loaded into the RNA-induced silencing complex (RISC) and then the duplex is matured (Treiber et al., 2019). Importantly, two distinct functional mature miRNAs can be processed from opposite sides of the same pre-miRNA (i.e., miRNA matured from the 5′ arm denoted -5p or from the 3′ arm denoted -3p) (Treiber et al., 2019). Finally, the miRNA-RISC (miRISC) is guided by a seed sequence (spanning position 2 to 8 at the 5′ end of the miRNA) that base pairs to a specific miRNA recognition element (MRE) typically harbored in the 3′-untranslated region (3′-UTR) of a target mRNA (Bushati and Cohen, 2007). Interactions of miRNAs with the 5′-untranslated region (5′-UTR) and coding region of mRNAs have also been reported (Broughton et. al., 2016). Upon

mRNA binding, miRISC will reduce the expression of the target mRNA by blocking the ribosome from mRNA translation and/or by initiating mRNA degradation (Fabian and Sonenberg, 2012; Jonas and Izaurralde, 2015).

In this study, we posit that TOP2α/170 expression is attenuated in etoposide resistant K/VP.5 cells, in part, by miRNA-mediated mechanisms that are determinants of drug resistance. Results demonstrated that human miR-9-3p (previously denoted miR-9*) and miR-9-5p (previously denoted miR-9) were: 1) overexpressed in K/VP.5 cells; 2) contained corresponding MREs in the 3′-UTR of TOP2α/170: 3) functionally regulated the protein expression levels of TOP2α/170; 4) modulated etoposide activity. Together results are consistent with a role for these miRNAs in acquired drug resistance.

Materials and Methods

Cell Culture. Human K562 leukemia cells were maintained in Dulbecco's modified Eagle's medium (DMEM) (Corning, Manassas, VA) supplemented with 10% fetal bovine serum (FBS). Cloned etoposide resistant K562 cells (K/VP.5) were generated by continuous incubation in 0.5 µM etoposide followed by isolation via limiting dilution, as previously described (Ritke and Yalowich, 1993). K/VP.5 cells were maintained in DMEM/10% FBS with 0.5 µM etoposide added every other week. All experiments described below were performed utilizing K562 and K/VP.5 cells growing in log phase.

miRNA-Sequencing. A mirVana miRNA Isolation Kit with phenol was used to isolate total RNA from K562 and K/VP.5 cells following the manufacturer's recommended instructions (cat # AM1560; ThermoFisher, Waltham, USA). The total RNA was subsequently DNase I treated and concentrated on a spin-column following the manufacturer's recommended instructions (cat # R1013; Zymo Research, Irvine, CA, USA). miRNA-Seq analysis was performed by the Biomedical Genomics Core of The Research Institute at Nationwide Children's Hospital, Columbus, Ohio. Briefly, NEB Next Small RNA libraries were prepared form the purified K562 and K/VP.5 total RNA samples and the libraries were size selected using Sage Pippin (130-200 bp range, adapters are ~128 bp) with an average final library size of 180 bp and sequenced on MiniSeq as 2 x 75 bp reads.

Computational processing of smRNA-seq data. First, 3′ adaptor sequences and low quality bases were trimmed from 75 base pair paired-end sequence reads using Cutadapt v2.4 (Martin, 2011). Trimmed reads with a sequence length between 15 and 50 base pairs were aligned to potential contaminant sequences of human genome (ribosomal RNAs and tRNAs) using Bowtie v1.1.2 (Langmead et al., 2009) with a seed length of 18 and allowing zero mismatches in the seed.

Then, remaining reads were aligned to miRbase (Griffiths-Jones, 2004) v21 mature sequences using Bowtie v1.1.2 with a seed length of 18, allowing 1 mismatch in seed and reporting maximum 5 alignments per read. Finally, remaining reads were aligned to human reference genome, GRCh38, using Bowtie v1.1.2 with a seed length of 18, allowing 1 mismatch in seed and reporting only unique alignments for each read. Using Samtools (Li et al., 2009) and in-house R scripts, total number of reads for each mature miRNA was counted. Fractional counts were used when a sequence read aligns to more than one miRNA. Genomic alignment was quantified using featureCounts function of SubReads (Liao et al., 2014) with Gencode v22 annotation. Using limma R/Biconductor package (Ritchie et al., 2015), raw read counts were normalized as log2 counts per million (CPM) and differential expression analysis was performed between three K562 and four K/VP.5 RNA samples.

TOP2α/170 mRNA/miRNA Bioinformatic Analyses. To predict putative MREs harbored in the 3'-UTR of TOP2α/170 mRNAs, multiple computational algorithms were utilized (TargetScan 7.2, http://www.targetscan.org; Agarwal et al., 2015 and DIANA-microT-CDS, http://www.microrna.gr/microT-CDS, 5th version of the microT algorithm, Paraskevopoulou et al., 2013).

Luciferase Reporter Constructs. The psiCHECK-2 dual luciferase vector was purchased from Promega Corporation (cat # C8021; Madison, WI, USA) and linearized by XhoI digestion (cat # R0146S; New England Biolabs, Ipswich, MA, USA) according to the manufacturer's protocol. A 998-bp fragment encompassing the entire TOP2α/170 3′-UTR was PCR amplified by utilizing sense (5′-AGGCGATCGCTCGAG**AATGTGAGGCGATTATTTTAAGTAA**-3′) and antisense (5′-ATTCCCGGGCTCGAG**TGGGTTGCAATGTTTAGAACATT**-3′) primers using standard PCR procedures with a proofreading polymerase, CloneAmp HiFi (cat # 639298; Takara Bio Inc.,

9

Kusatsu, Shiga, Japan). Genomic DNA isolated from K562 cells was used as template. The primer sequences homologous to the regions immediately downstream of the TOP2α/170 stop codon and immediately upstream of the TOP2α/170 poly(A) tail are bolded above. The sense and antisense primers also harbor 15 nucleotide extensions (not bolded) that are homologous to ends of the XhoI linearized dual luciferase psiCHECK-2 reporter plasmid and are necessary for "In-Fusion" cloning methodology (In-Fusion HD Cloning Kit, cat # 638916; Takara Bio Inc). The TOP2α/170 3′-UTR PCR product was gel purified and subcloned into the XhoI site which is located downstream of the Renilla luciferase (r-luc) reporter open reading frame in the psiCHECK-2 reporter plasmid utilizing the manufacturer's protocol. The authenticity and orientation of the inserts relative to the Renilla luciferase gene were confirmed by dideoxy sequencing. The resulting recombinant plasmid was designated psiTOP2α/170/UTR.

The mutant reporter construct psiTOP2α/170/UTR-mut-5p was generated utilizing the psiTOP2α/170/UTR vector as template and mutating the miR-9-5p MRE (located at 703-709 bp) harbored in the TOP2α/170 3′-UTR using a Q5 Site-Directed Mutagenesis kit from New England Biolabs (cat # E0554S) following the manufacturer's instructions. The primers utilized for mutagenesis were sense (5′-**AAGCGTG**GAGAAACCAATTTCTAAG-3′) and antisense (5′-GAGATTCAGACTCAGAGGCAGC-3′). Importantly, these primers were designed with their 5′ ends annealing back-to-back (inverse PCR). The nucleotides that were mutated are shown in bold print. The mutation of the miR-9-5p seed sequence was confirmed by dideoxy sequencing. The mutant reporter construct psiTOP2α/170/UTR-mut-3p was generated in the same manner as psiTOP2α/170/UTR-mut-5p, but at (466-471 bp of the 3′-UTR) with the following sense (5′-**GAAACT**GGTTCTAGTACAGATAC-3′) and antisense (5′-TTCTATCTGATGGTAAA-TTATG-3′) primers. Finally, transformed bacterial cultures were grown and each reporter construct was isolated with a Qiagen Plasmid Midi Kit (cat # 12143; Hilden, Germany).

10

Transfection Experiments. K562 and K/VP.5 cells (5 x 10^5 in 5 mL per condition) were transfected with the psiTOP2α/170/UTR dual luciferase construct utilizing 1 µg of the plasmid, 5.5 µl Lipofectamine 3000, 10 µl P3000 (cat # L3000008; ThermoFisher), and 250 µl Opti-Mem Medium (cat # 31985062; ThermoFisher). Co-transfection experiments utilizing K562 cells were performed as described above with the respective dual luciferase construct (psiTOP2α/170/UTR, psiTOP2α/170/UTR-3p-mut, or psiTOP2α/170/UTR-5p-mut) and either a miRNA mimic negative control (cat # 4464058; ThermoFisher), miR-9-3p mimic (cat # MC13072), or miR-9-5p mimic (cat # MC10022). In addition, K562 cells were transfected with only the mimics described above for subsequent TOP2α/170 immuno-assays and for DNA damage studies. Finally, K/VP.5 cells were transfected with either a miRNA inhibitor negative control (cat # MH4464076, ThermoFisher), miR-9-3p inhibitor (cat # MH13072), or miR-9-5p inhibitor (cat # MH10022). In all transfection experiments employing miRNA mimics or miRNA inhibitors the final concentration was 25 nM. Forty-eight hr after transfection, total RNA and/or cellular extracts were prepared for qPCR, luciferase, immunoblotting and DNA damage assays as outlined below.

Quantitative PCR (qPCR) Assays. Total RNA was isolated from non-transfected and transfected K562 and K/VP.5 cells using PureZOL RNA Isolation Reagent from Bio-Rad Laboratories (cat # 7326880; Hercules, CA, USA). RNA samples were subsequently treated with DNAse I (TURBO DNA-free Kit, cat # AM2238, ThermoFisher Scientific). RNA (1µg) utilized for TOP2α/170 mRNA quantification experiments was reverse transcribed using random hexamers and MultiScribe Reverse Transcriptase (High Capacity cDNA Reverse Transcription Kit, cat # 4368814; ThermoFisher Scientific) as previously described by our laboratory (Kanagasabai, et al., 2017; Kanagasabai, et al., 2018). qPCR evaluations (20 µl/reaction) were performed using 5 µl of a 1:10 dilution of cDNA with primer/probe sets specific for TOP2α/170 (Assay ID Hs01032135_m1; ThermoFisher Scientific) and TATA-box binding protein (TBP) (Assay ID

11

Hs99999910_ml; ThermoFisher Scientific). The relative gene expression level of TOP2α/170 in each experimental condition was normalized to TBP expression using the $2^{-\Delta\Delta Ct}$ method (Schmittgen and Livak, 2008). In addition, RNA samples (50 ng) were reverse transcribed using miR-9-3p, miR-9-5p, and RNU48 antisense primers and MultiScribe Reverse Transcriptase in a 15 µl reaction according to manufacturer instructions. qPCR for miRNA quantification (20 µl/reaction) was performed using 1.33 µl of cDNA with primer/probe sets specific for miR-9-3p (Assay ID 00231), miR-9-5p (Assay ID 000583), and RNU48 (Assay ID 001006). The relative gene expression level of miR-9-3p and/or miR-9-5p in each experimental condition was normalized to RNU48 expression using the $2^{-\Delta\Delta Ct}$ method (Schmittgen and Livak, 2008). Finally, cDNA synthesized from RNA isolated from non-transfected K562 and K/VP.5 cells was utilized in qPCR experiments with primer/probe sets specific for primary (pri) hsa-miRNA-9s (mir-9-1, Assay ID Hs03303201_pri; mir-9-2, Assay ID Hs03303202_pri; and mir-9-3, Assay ID Hs03293595_pri; ThermoFisher Scientific). The relative gene expression level of mir-9-1, mir-9-2, and mir-9-3 in K562 and K/VP.5 cells was normalized to TBP expression using the $2^{-\Delta\Delta Ct}$ method (Schmittgen and Livak, 2008).

Luciferase Assay. Forty-eight hr after transfection, K562 and/or K/VP.5 cells were washed and lysed with passive lysis buffer (cat # E1941; Promega), and firefly and Renilla luciferase activities were determined by using the Dual-Luciferase Reporter Assay System (cat # E1910; Promega) with a Synergy H1 Hybrid Multi-Mode Reader (BioTek, Winooski, VT, USA). Renilla luciferase expression in the psiCHECK-2 vector is generated via an SV40 promoter while firefly luciferase in this vector is generated via a HSV-TK promoter and has been specifically designed to be an intraplasmid transfection normalization reporter. The Renilla luciferase signal was therefore normalized to the firefly luciferase signal.

Western Blot Analysis. Forty-eight hr after transfection, K562 and/or K/VP.5 cells were pelleted and washed in phosphate-buffered saline (PBS). After washing, 1.5 million cells were lysed in 2x Laemmli sample buffer (cat # 1610737; Bio-Rad Laboratories) containing 5% β-mercaptoethanol, and boiled at 100 °C for 5 min. DNA was sheared using a sonicator (Tekmar, Mason, OH, USA) at 35 W three times in 10 second intervals and the samples were subsequently electrophoresed on a NuPAGE 4-12% Bis-Tris gel (cat # NP0322BOX; ThermoFisher). Duplicate samples were run with an equal amount of protein (16.6 µg) loaded into each well and an equal volume of Precision Plus Protein Dual Color Standards were also run for molecular weight reference (cat # 1610374; Bio-Rad Laboratories). Protein was transferred to a polyvinylidene difluoride (PVDF) membrane (cat# 1620177; Bio-Rad Laboratories) using a semidry electroblotter (ThermoFisher). The PVDF membrane was then sectioned. The 75-250 kDa portion was labeled by overnight incubation at 4 °C with rabbit polyclonal antibodies raised against the N-terminal sequence of human TOP2α/170 (cat. No. ab74715; Abcam, Cambridge, MA; used at 1:1000 dilution). The 25-75 kDa portion was labeled by overnight incubation at 4 °C with a glyceraldehyde 3-phosphate dehydrogenase (GAPDH) mouse monoclonal antibody (1:5000; cat # sc-47724; Santa Cruz Biotechnology, Santa Cruz, CA). PVDF membranes were subsequently incubated at room temperature for 1.5 hr with a donkey anti-rabbit or donkey anti-mouse secondary antibody respectively (1:8000 dilution; Jackson ImmunoResearch, West Grove, PA). Antibody-labeled TOP2α/170 and GAPDH were detected using the Immun-Star horseradish peroxidase Chemiluminescence Kit (cat # 170-5040; Bio-Rad Laboratories). All immunoassay images were taken with the ChemiDoc XRS+ imaging system and analyzed with ImageLab software (Bio-Rad Laboratories).

Comet DNA Damage Assays. Single-cell gel electrophoresis (Comet) assays were performed according to the manufacturer's protocol (cat # 4250-050-K; Trevigen, Gaithersburg, MD) and as previously described by our laboratory (Vlasova, et al., 2011; Kanagasabai, et al., 2017). Briefly,

K562 or K/VP.5 cells were transfected with miR-9 mimics or inhibitors respectively as described above. Forty-eight hr after transfection, cells were washed and resuspended in buffer (25mM HEPES, 10 mM glucose, 1 mM $MgCl_2$, 5 mM KCl, 130 mM NaCl, 5 mM NaH2PO4, pH 7.4). Transfected K562 cells were subsequently incubated with 2 or 5 µM etoposide or DMSO (solvent control) for 1 hr at 37 °C. Transfected K/VP.5 cells were incubated with 10 or 25 µM etoposide or DMSO for 1 hr at 37 °C. Cells were subsequently washed with ice-cold buffer and resuspended to 0.28×10^6 cells/ml and subsequently diluted so that ~2000 cells in low melt agarose underwent alkaline electrophoresis. After staining with a fluorescent DNA intercalating dye, SYBR Gold, the migrating fragments (comet tail) from the nucleoid (comet head) were visualized and the images captured by fluorescence microscopy. The Olive tail moment, which is defined as the product of the comet tail length and the fraction of total DNA in the comet tail (Olive, 2002), was quantified by the ImageJ processing program with the open-source software tool Open Comet (Gyori, et al., 2014). Olive tail moments from greater than 100 cells per sample condition were determined.

Data Analysis. Statistical analysis was performed using SigmaPlot 14. All data are expressed as the mean ± S.D. Group-wise differences were analyzed using a two-tailed paired Student's t-test with no correction for multiple comparisons. qPCR gene expression data $(2^{-\Delta Ct}$ values) were subjected to log transformation to assure distribution normality prior to paired Student's t-test analysis (Ganger et. al. 2017). A P-value < 0.05 was considered statistically significant.

Results

TOP2α/170 Expression is Attenuated in Etoposide (VP-16) Resistant K562 cells. Our laboratory previously established and characterized an etoposide resistant K562 cell line, designated K/VP.5 cells (Ritke and Yalowich, 1993), cross-resistant also to other TOP2α/170 targeted agents (Ritke et al., 1994). To demonstrate resistance to etoposide, cell growth inhibition of K562 and K/VP.5 cells was evaluated by 48 hr incubation with increasing concentrations of etoposide. Results show that K/VP.5 cells are 26-fold resistant to etoposide (Fig. 1A). To investigate the relative TOP2α/170 mRNA expression levels, K562 and K/VP.5 cDNAs were subjected to qPCR utilizing TaqMan hydrolysis primers/probes. The results of these experiments demonstrated that TOP2α/170 mRNA expression levels were reduced in K/VP.5 cells to 41.2% the level expressed in parental K562 cells (Fig. 1B); recapitulating the 2.5-fold reduction of TOP2α/170 mRNA in K/VP.5 cells found previously by Northern blot analysis (Ritke and Yalowich, 1993). TOP2α/170 protein expression was also decreased in K/VP.5 cells to a level 10.6% that of parental K562 cells (Fig. 1C).

miR-9-3p and miR-9-5p are Overexpressed in K/VP.5 Cells. Since miRNAs play an integral role in almost all known biological processes (reviewed in Bushati and Cohen, 2007; Bartel, 2009; Fabian and Sonenberg, 2012), we hypothesized that TOP2α/170 expression is attenuated in K/VP.5 cells, in part, by a miRNA-mediated mechanism. As an initial test of this hypothesis, total mRNA was isolated from K562 and K/VP.5 cells and small RNA libraries were generated, size selected, and sequenced to examine the global miRNA expression levels in both cell lines. The volcano plot (Fig. 2A) illustrates that, of the ~300 mature miRNAs that were detected in these cells, 73 miRNAs were overexpressed (fold change > 2; adjusted *P*-value < 0.05) and 14 were underexpressed (fold change > 2; adjusted *P*-value < 0.05) in K/VP.5 compared to K562 cells

The miRNA-Seq data demonstrated that miR-9-3p (75.1-fold) and miR-9-5p (26.2-fold) were among the top six overexpressed pre-miRNAs in K/VP.5 cells (Fig. 2A). TargetScan (Agarwal et al., 2015) and DIANA-microT-CDS (Paraskevopoulou et al., 2013) algorithms identified a putative mature miR-9-5p MRE located at position 703-709 nt in the TOP2α/170 3′-UTR (Fig. 2B). In addition, a putative seed sequence for miR-9-3p binding was predicted manually at position 466-471 nt of the TOP2α/170 3′-UTR (Fig. 2B). Based on these evaluations, and literature establishing that miR-9-3p and miR-9-5p can be simultaneously matured from pre-miR (mir-9) (Packer et al., 2008; Schraivogel et al., 2011, Nowek et al., 2016, 2018), the potential effects of both these miRNAs were studied further.

To independently validate the miR-9 miRNA-Seq data (Fig. 2A), qPCR experiments were performed utilizing TaqMan primer/probe sets specific for mature miR-9-3p and miR-9-5p. Both miR-9-3p and miR-9-5p were statistically significantly overexpressed in K/VP.5 cells compared to K562 cells; 18.6-fold and 12.7-fold, respectively; $P < 0.001$ (Fig. 2C). Since miR-9-3p and miR-9-5p can be matured from pri-miRNAs (mir-9s) transcribed from three independent genes; MIR9-1, MIR9-2, and MIR9-3 located on chromosomes 1, 5, and 15 respectively (Yuva-Aydemir et al., 2011), qPCR experiments were performed utilizing TaqMan primer/probe sets specific for each MIR9 gene. These experiments demonstrated that mir-9-1 was the only miRNA precursor statistically significantly overexpressed in K/VP.5 cells compared to K562 cells (18.6-fold; $P < 0.001$) (Fig. 2D). Together these observations suggest that it is the activation of the MIR9-1 gene that results in the overexpression of miR-9-3p and miR-9-5p in K/VP.5 cells.

miR-9-3p and miR-9-5p Directly Interact With the TOP2α/170 3′-UTR. Initial evaluation of putative miRNA regulation of TOP2α/70 expression utilized a dual luciferase reporter assay system in which binding of a given miRNA to its distinct MRE may repress reporter

protein production, thereby reducing Renilla-luc activity (Kuhn et al., 2008; Sansom et al., 2010; Elton and Yalowich 2015). Therefore, the TOP2α/170 3′-UTR (998-bp), which harbored MREs for miR-9-3p and miR-9-5p (Fig. 2B), was subcloned immediately downstream of the Renilla-luc open reading frame and the plasmid construct was designated psiTOP2α/170/UTR. After transfection of cells with psiTOP2α/170/UTR, there was a statistically significant reduction in luciferase activity in K/VP.5 compared to K562 cells ($P < 0.001$) suggesting a miRNA-mediated mechanism regulating TOP2α/170 protein expression levels (Fig. 3A).

To evaluate the putative role of miR-9-3p and/or miR-9-5p in this regulation, K562 cells, which express low levels of miR-9-3p and miR-9-5p, were cotransfected with the psiTOP2α/170/UTR construct (1 μg) plus 25 nM miR-9-3p, miR-9-5p, or control non-targeting miRNA mimics (chemically modified double-stranded RNAs that mimic endogenous miRNAs) for gain-of-inhibitory-function experiments. Forty-eight hr after transfection, qPCR experiments utilizing TaqMan probes specific for miR-9-3p or miR-9-5p demonstrated that transfection with the corresponding miRNA mimic significantly increased the detectable levels of miR-9-3p (600-fold) and miR-9-5p (94-fold), $P < 0.001$ for both (Fig. 3B). No significant increase was observed for miR-9-5p after miR-9-3p mimic transfection nor was there a statistically significant increase in miR-9-3p after mir-9-5p mimic transfection, $P > 0.220$ for both (Fig. 3B); demonstrating the specificity of miR-9 mimics and the qPCR assays. K562 cells were cotransfected with psiTOP2α/170/UTR and miR-9 mimics followed by measurement of luciferase activity 48 hr later (Fig. 3C). There was a statistically significant reduction in luciferase activity to 71.4% ($P = 0.033$) and 42.1% ($P = 0.001$) of the non-targeted miR-9 mimic control, in cells treated with miR-9-3p mimic and miR-9-5p mimic, respectively (Fig. 3C).

To validate that miR-9-3p and miR-9-5p interact with the predicted MREs harbored in the 3′-UTR of TOP2α/170 mRNA, additional luciferase reporter constructs were generated where the MRE "seed" sequences (CUUUAU for miR-9-3p and CCAAAGA for miR-9-5p), which are complementary to the 5′ ends of miR-9-3p and miR-9-5p, were mutated (GAAACU for miR-9-3p and AAGCGUG for miR-9-5p) (Fig. 3D bottom). The mutant constructs were designated psiTOP2α/170/UTR-mut-3p and psiTOP2α/170/UTR-mut-5p. Co-transfection of K562 cells (48 hr) with psiTOP2α/170/UTR-mut-3p plus miR-9-3p mimic or with psiTOP2α/170/UTR-mut-5p plus miR-9-5p mimic revealed that, compared to wild-type psiTOP2α/170/UTR transfection results (Fig. 3C), these miRNAs no longer had any effect on luciferase activity (Fig. 3D). Together, results from Figs. 3C and 3D indicate that miR-9-3p and miR-9-5p can interfere with luciferase expression by directly interacting with the predicted miR-9-3p and miR-9-5p MREs harbored within the 3′-UTR TOP2α/170 mRNA.

miR-9-3p and miR-9-5p Overexpression Results in Decreased TOP2α/170 Protein and Reduced Etoposide-induced DNA Damage in K562 Cells. If TOP2α/170 mRNA is a biological target of miR-9-3p and miR-9-5p, alteration of the endogenous expression levels of these miRNAs should correspond to predictable changes in TOP2α/170 protein. Therefore, additional gain-of-inhibitory-function experiments were performed by transfecting K562 cells (48 hr) with 25 nM miR-9-3p, miR-9-5p, or control (non-targeting) miRNA mimics followed by immunoblotting of cell lysates to evaluate TOP2α/170 protein levels. Fig. 4A shows that TOP2α/170 levels were similar in mock transfected (lipofectamine only) and miRNA mimic control conditions (Fig. 4A). Consistent with our hypothesis, TOP2α/170 protein levels were decreased when miR-9-3p or miR-9-5p were overexpressed (Fig. 4A). Averaging results from five separate experiments run on separate days, there was a reduction of TOP2α/170 levels to 67.6% ($P < 0.001$) and 49.6% ($P =$

18

0.004), of miRNA mimic control, in cells treated with miR-9-3p and miR-9-5p, respectively (Fig. 4B).

Etoposide-induced DNA damage correlates most often with levels of the target type II Topoisomerases (Ritke and Yalowich, 1993; Ritke et al, 1994; Mirski et al., 1993, 2000; Harker et al., 1995; Mirski and Cole, 1995; Wessel et al., 1997; Yu et al., 1997; Burgess et al., 2008; Ganapathi and Ganapathi, 2013). Hence, we next investigated whether forced expression of miR-9-3p and miR-9-5p would diminish etoposide activity in parallel with a reduction in TOP2α/170 levels (as demonstrated in Figs. 4A and 4B). K562 cells were transfected with 25 nM miR-9-3p, mir-9-5p, or non-targeting control miRNA mimics. Forty-eight hr after transfection, cells were incubated for 1 hr with etoposide (2 or 5 μM) or DMSO vehicle and subsequently evaluated for DNA damage by alkaline single cell gel electrophoresis (Comet) assays (Kanagasabai et al., 2017; Kanagasabai et al., 2018). Etoposide-induced DNA strand breaks were attenuated in miR-9-3p and miR-9-5p mimic transfected K562 cells compared to control miR-mimic (Fig. 4C). Averaging results from 7 experiments run on separate days, there was a reduction in; 1) etoposide (2 μM)-induced DNA damage to 59.7% ($P = 0.011$) and 70.7% ($P = 0.025$) of control; 2) etoposide (5 μM)-induced DNA damage to 80.7% ($P = 0.006$) and 77.4% ($P = 0.002$) of control, in K562 cells transfected with miR-9-3p or mir-9-5p mimics, respectively (Fig. 4C). Together these results indicate that forced overexpression of miR-9-3p or miR-9-5p reduces TOP2α/170 protein expression and, as a consequence, decreases etoposide-mediated DNA damage.

The potential mechanism by which miR-9-3p and miR-9-5p mimics reduce TOP2α/170 protein levels was assessed by qPCR. RNA isolated from miR-9-3p and mir-9-5p mimic transfected K562 cells was utilized to quantify TOP2α/170 mRNA levels. Transfection with miR-9-3p or miR-9-5p mimics did not alter TOP2α/170 steady-state mRNA levels (Fig. 4D). Therefore,

19

decreased TOP2α/170 protein expression observed in K562 cells by forced expression of miR-9-3p and miR-9-5p is not due to the degradation of TOP2α/170 mRNA suggesting that these miRNAs/miRISC function by blocking the ribosome from translating TOP2α/170 mRNA.

miR-9-3p and miR-9-5p Inhibitors Increase TOP2α/170 Protein and DNA Damage in K/VP.5 Cells. Since the miR-9-3p and miR-9-5p forced expression (gain-of-inhibitory-function) experiments described (Fig. 4) may lead to off-target effects due to supra-physiological miRNA levels (Fig. 2C) (Bracken et al., 2008; Khan et al., 2009), reciprocal loss-of-miR-9-inhibitory-function experiments were also performed in K/VP.5 cells. Utilizing miRNA inhibitors (chemically modified single stranded antisense nucleic acids designed to bind to and inhibit miRNA function), effects on TOP2α/170 protein expression and subsequent etoposide-induced DNA damage were evaluated. K/VP.5 cells, which express high levels of miR-9-3p and miR-9-5p (Fig. 2B), were transfected with 25 nM miR-9-3p, miR-9-5p, or control miRNA inhibitors (48 hr) followed by immunoblotting of cell lysates to evaluate TOP2α/170 protein levels. Fig. 5A shows that TOP2α/170 protein in K/VP.5 cells was increased after transfection of miR-9-3p and miR-9-5p inhibitors. Averaging results from 5 separate experiments run on separate days, there was an increase in TOP2α/170 levels to 261% ($P = 0.035$) and 256% ($P = 0.027$) of miRNA inhibitor control in K/VP.5 cells treated with miR-9-3p inhibitor and miR-9-5p respectively (Fig. 5B).

We next investigated whether transfection of K/VP.5 cells with miR-9-3p and miR-9-5p inhibitors would increase etoposide activity in parallel with the increase in TOP2α/170 protein levels (as demonstrated in Figs. 5A and 5B). K/VP.5 cells were transfected with 25 nM miR-9-3p, miR-9-5p, or control miRNA inhibitors. Forty-eight hr after transfection, cells were incubated for 1 hr with etoposide (10 or 25 μM) or DMSO vehicle and subsequently evaluated for DNA damage

by alkaline single cell gel electrophoresis (Comet) assays (Kanagasabai et al., 2017; Kanagasabai et al., 2018) as above in Fig. 4C. Averaging results from 6 separate experiments performed on separate days, there was an increase in: 1) etoposide (10 µM)-induced DNA damage to 183% (P = 0.004) and 163% (P = 0.026) of control; 2) etoposide (25 µM)-induced DNA damage to 119% (P = 0.040) and 130% (P = 0.008) of control, in K/VP.5 cells transfected with miR-9-3p or miR-9-5p inhibitors, respectively (Fig. 5C). Together results indicate that miR-9-3p and miR-9-5p inhibitors allow for increased TOP2α/170 protein expression in drug resistant K/VP.5 cells and, as a consequence, enhanced etoposide-induced DNA damage.

Similar to results in miR-9-mimic transfected K562 cells (Fig. 4D), neither miR-9-3p nor miR-9-5p inhibitor elicited changes in TOP2α/170 mRNA when transfected in K/VP.5 cells (Fig. 5D), again suggesting that miR-9 effects are not related to alteration in mRNA stability but may impact on translation of TOP2α/170 mRNA; in this case by loss of miR-9-3p and miR-9-5p inhibitory activity.

Discussion

Acquired drug resistance is a major therapeutic challenge in the treatment of cancers. Chemoresistance can result from a number molecular mechanisms including aberrant drug transport/trafficking processes, altered drug metabolism, increased or modified drug targets, abnormal cell cycling, cell death evasion, and DNA damage/repair dysregulation (Zahreddine and Borden, 2013; Cree and Charlton, 2017). In recent years, numerous studies have shown that miRNAs can be involved in acquired drug resistance by directly targeting mRNAs which encode proteins regulating the biological pathways described above (Gabra and Salmena, 2017; Anfossi et al., 2018; Corra et al., 2018). Our present study focused on whether decreased TOP2α/170 levels (Fig. 1C) and attenuated etoposide activity in K/VP.5 cells (Fig. 1A) result, in part, from miRNA mechanisms.

miRNA-Seq data revealed that 73 mature miRNAs were overexpressed and 14 miRNAs were repressed in K/VP.5 cells compared to K562 cells (Fig. 2A). Algorithm searches (Agarwal et al., 2015; Paraskevopoulou et al., 2013) suggested that of the 73 overexpressed miRNAs in K/VP.5 cells, nine miRNAs were predicted to interact with MREs harbored within the TOP2α/170 mRNA (not shown). miR-9-3p and miR-9-5p were highly overexpressed in K/VP.5 cells (Fig. 2A) and MREs were identified in the TOP2α/170 3′-UTR (Fig. 2B) for both these miRNAs, leading to further investigation of their function(s).

During RISC loading, the miRNA duplex is bound by a member of the Argonaute (AGO) protein family followed by strand selection (Treiber et al., 2019). Typically, the strand with the least thermodynamically stable base pair at its 5′ end in the miRNA duplex is selected as the guide strand. The "passenger" strand with the stronger 5′ end interaction is released and degraded (Schwarz et al., 2003; Khvorova et al., 2003). However, the passenger strand can also be loaded

22

into the miRISC and exhibit inhibitory activity like any other miRNA (Packer et al., 2008). The ratio of AGO-loaded 5p or 3p mature strand varies greatly, with co-expression of 5p/3p pairs demonstrated in about half of the miRNA populations analyzed (Ro et al., 2007; Kuchenbauer et al., 2011). Such seems to be the case with miR-9-3p and miR-9-5p in K562 and K/VP.5 cells.

Using qPCR, we confirmed miRNA-Seq data (Fig. 2A) to demonstrate overexpression of both miR-9-3p (18.6-fold) and miR-9-5p (12.7-fold) in K/VP.5 compared to K562 cells (Fig. 2C). Additionally, transfection of luciferase constructs containing TOP2α/170 3′-UTR established that TOP2α/170 mRNA is a direct target of both miRNAs (Figs. 3C-D). Transfection of miR-9 inhibitors increased TOP2α/170 expression and enhanced etoposide-induced DNA damage in resistant K/VP.5 cells while forced overexpression of both miRNAs in parental K562 cells decreased TOP2α/170 levels and reduced etoposide activity (Figs. 4-5). Since decreased TOP2α/170 expression is most often associated with resistance (Ganapathi and Ganapathi, 2013), our results strongly suggest that increased expression of miR-9-3p and miR-9-5p in K/VP.5 cells are determinants of acquired resistance.

Consistent with our observations of dual expression/function of miR-9-3p and miR-9-5p, both miRNAs cooperate in regulating the balance between self-renewal and differentiation of human neural stem cells by simultaneously targeting members of the notch pathway (Roese-Koerner, et al., 2016). Additionally, miR-9-3p and miR-9-5p can be co-expressed in primary cases of human acute myeloid leukemia (AML) and co-target ETS-related gene mRNA (Nowek et al., 2016). Finally, miR-9-3p and miR-9-5p concurrently target calmodulin binding transcription activator 1 mRNA in glioblastoma stem cells (Schraivogel et al., 2011).

Importantly, dysregulation of miR-9-3p and/or miR-9-5p expression has been implicated in a wide range of diseases including cancers (Nass et al., 2009; Barbano et al., 2017; Nowek et

al., 2018), diabetes (Chakraborty et al., 2014), neurodegenerative diseases (Packer et al., 2008; Juzwik et al., 2019), osteoarthritis (Nugent 2016), and sporadic premature aging syndromes (Frankel et al., 2018).

Increased levels of miR-9-3p and/or miR-9-5p have been shown to play an important role in mediating chemoresistance (Munoz et al., 2013, 2015a, 2015b). In temozolomide resistant glioblastoma cells: 1) miR-9-3p and miR-9-5p were overexpressed (Munoz et al., 2015a); 2) miR-9-5p led to increased expression of ABCB1 through activation of the Sonic Hedgehog (SHH) pathway (Munoz et al., 2015b); 3) delivery of anti-miR-9-5p decreased ABCB1 and sensitized resistant glioblastoma cells to temozolomide (Munoz et al., 2013).

Conversely, Li et al. (2017) demonstrated that miR-9-3p expression was significantly reduced in Adriamycin (ADR) resistant K562/ADR compared to parental K562 cells. These investigators also established that miR-9-3p targeted ABCB1 and that transfection of miR-9-3p mimics increased the chemosensitivity of K562/ADR cells. Li et al. (2015) demonstrated that miR-9-5p was downregulated in both paclitaxel resistant epithelial ovarian carcinoma (EOC) patient samples and EOC cell lines. Similarly, Sun et al. (2013) established that cisplatin resistant ovarian cancer patients manifest lower miR-9-5p expression levels. In AML cell lines resistant to daunorubicin (DNR), transfection of miR-9-5p mimics enhanced chemosensitivity to DNR by targeting eukaryotic translation initiation factor 5A-2 (Liu et al., 2019). Collectively, this literature indicates that over- or underexpression of miR-9-3p or miR-9-5p can play a critical role in chemoresistance depending on cell type. Additionally, these observations support the conclusion that miR-9-3p and/or miR-9-5p act on many mRNA targets important in chemoresistance.

miRISC mediates post-transcriptional silencing of specific mRNAs that contain MREs that are partially or fully complementary to the miRNA (Bartel, 2009). Silencing occurs by target

mRNA translational repression and/or mRNA degradation (Fabian and Sonenburg, 2012; Jonas and Izaurralde, 2015). Ribosome profiling studies which compared changes in translational efficiency to changes in mRNA levels, demonstrated that the majority of the negative post-transcriptional gene regulatory effects of miRNAs/miRISCs resulted from mRNA degradation (Guo et al., 2010; Eichhorn et al., 2014); true translational repression accounts for only 6–26% of the decrease of each endogenous target in mammalian cells (Eichhorn et al., 2014).

Our studies demonstrated that there was no reduction in TOP2α/170 steady-state mRNA levels after transfection of K562 cells with miR-9-3p or miR-9-5p mimics (Fig. 4D), which attenuated TOP2α/170 protein levels (Fig. 4A-B), or after transfection of K/VP.5 cells with miR-9-3p or miR-9-5p inhibitors (Fig. 5D), which increased TOP2α/170 protein levels (Fig. 5A-B). These results strongly suggest that TOP2α/170 mRNA is translationally repressed by these miRNAs. In contrast, Hua et al., 2015 demonstrated that TOP2α/170 mRNA (and protein) was reduced by miR-139 in luminal type breast cancer cells, again pointing to the pleiotropic effects of miRNAs.

Though we conclude that miR-9-3p and miR-9-5p impact translation, steady-state mRNA levels of TOP2α/170 are reduced in K/VP.5 compared to K562 cells (Fig. 1B) attributable to alternative RNA processing of TOP2α/170 pre-mRNA, as we have reported previously (Kanagasabai et al., 2017; Kanagasabai et al., 2018). Hence, reduced TOP2α/170 protein levels (and acquired drug resistance) can derive from both translational repression (via miRNA mechanisms) and aberrant pre-mRNA processing.

Given that three distinct MIR9 genes transcribe primary transcripts processed into identical mature miR-9-3p and miR-9-5p miRNAs (Yuva-Aydemir et al., 2011), we performed qPCR experiments to investigate whether MIR9-1, MIR9-2, MIR9-3, or a combination of these genes

25

were significantly upregulated in etoposide resistant K/VP.5 cells. Interestingly, only pri-miR-9-1 was significantly upregulated in K/VP.5 cells (Fig. 2D); likely leading to the observed increase in mature miR-9-3p and miR-9-5p expression levels.

It is not clear how MIR9-1 gene expression is activated in K/VP.5 cells. However, since the promoters of all three MIR9 genes are embedded within CpG islands, they are frequently aberrantly hypo- or hypermethylated in cancer (Kunej et al., 2011; Suzuki et al., 2013). Li et al. (2015) established that the MIR9-1 and MIR9-3 genes were hypermethylated in paclitaxel resistant EOC cell lines suggesting that decreased miR-9-5p expression resulted from aberrant DNA methylation. Recently, Fu et al. (2017) demonstrated that the MIR9-1 gene underwent heterochromatic silencing by the binding of the runt-related (RUNX) family transcription factor 1 (RUNX1) to the MIR9-1 promoter region and recruitment of chromatin-remodeling enzymes which resulted in the hypermethylation of MIR9-1 in t(8;21) AML. Given that RUNX1 is a direct target of both miR-9-3p and miR-9-5p (Tian et al., 2015; Raghuwanshi et al., 2018; TargetScan), we speculate that that the observed increase in MIR9-1 gene expression in etoposide resistant K/VP.5 cells may result from the hypomethylation of the MIR9-1 promoter due to decreased RUNX1 expression and the subsequent lack of recruitment of chromatin remodeling enzymes. Future experiments will test this hypothesis.

In conclusion, TOP2α/170 is an established therapeutic target, the expression levels of which are important for the efficacy of topoisomerase II-targeted drugs. Hence, it is critical to understand the mechanisms by which TOP2α/170 expression is regulated, especially in acquired drug resistance. Results demonstrated that miR-9-3p and miR-9-5p were overexpressed in etoposide resistant K/VP.5 cells and regulated the expression of TOP2α/170, likely through inhibition of translation. Additionally, miR-9-3p and miR-9-5p impact etoposide-induced DNA damage

26

secondary to effects on TOP2α/170 levels. This functional aspect of both miR-9-3p and miR-9-5p with regards to chemoresistance demonstrates their potential as drug targets for and/or biomarkers of resistance to TOP2α interfacial inhibitors.

Future studies aim to validate miR-9-3p and miR-9-5p as biomarkers of chemoresistance by analyzing expression in cells from newly diagnosed and relapsed leukemia patients who received TOP2α/170-targeted agents as well as establish the *in vivo* effects of these miRNAs on etoposide efficacy in xenograft models of leukemia.

Authorship Contributions
Participated in research design: Kania, Carvajal-Moreno, Hernandez, English, Papa, Ozer, Yalowich, Elton

Conducted experiments: Kania, English, Carvajal-Moreno, Hernandez, Papa, Shkolnikov

Contributed new reagents or analytical tools: Ozer, Kania,

Performed data analysis: Kania, Carvajal-Moreno, Hernandez, English, Papa, Shkolnikov, Ozer, Yilnaz, Yalowich, Elton

Wrote or contributed to the writing of the manuscript: Kania, Hernandez, Ozer, Elton, Yalowich

References

Agarwal V, Bell GW, Nam JW, and Bartel DP (2015) Predicting effective microRNA target sites in mammalian mRNAs. *Elife* **4:**10.7554/eLife.05005. eCollection 2015.

Anfossi S, Fu X, Nagvekar R, and Calin GA (2018) MicroRNAs, Regulatory Messengers Inside and Outside Cancer Cells. *Adv Exp Med Biol* **1056:**87-108.

Ashour ME, Atteya R, and El-Khamisy SF (2015) Topoisomerase-mediated chromosomal break repair: an emerging player in many games. *Nat Rev Cancer* **15:**137-151.

Barbano R, Pasculli B, Rendina M, Fontana A, Fusilli C, Copetti M, Castellana S, Valori VM, Morritti M, Graziano P, Luigi C, Coco M, Picardo F, Mazza T, Evron E, Murgo R, Maiello E, Esteller M, Fazio VM, and Parrella P (2017) Stepwise analysis of MIR9 loci identifies miR-9-5p to be involved in Oestrogen regulated pathways in breast cancer patients. *Sci Rep* **7:**45283.

Bartel DP (2009) MicroRNAs: target recognition and regulatory functions. *Cell* **136:**215-233.

Bracken CP, Gregory PA, Kolesnikoff N, Bert AG, Wang J, Shannon MF, and Goodall GJ (2008) A double-negative feedback loop between ZEB1-SIP1 and the microRNA-200 family regulates epithelial-mesenchymal transition. *Cancer Res* **68:**7846-7854.

Broughton JP, LovciMT, Huang JL, Yeo GW, and Pasquinelli AE (2016) Pairing beyond the Seed Supports MicroRNA Targeting Specificity. *Mol Cell* **64:**320-333.

Bugg BY, Danks MK, Beck WT, and Suttle DP (1991) Expression of a mutant DNA topoisomerase II in CCRF-CEM human leukemic cells selected for resistance to teniposide. *Proc Natl Acad Sci USA* **88:**7654-7658.

Burgess DJ, Doles J, Zender L, Xue W, Ma B, McCombie WR, Hannon GJ, Low SW, and Hemann MT (2008) Topoisomerase levels determine chemotherapy response in vitro and in vivo. *Proc Natl Acad Sci USA* **106:**9053-9058.

Bushati N and Cohen SM (2007) microRNA functions. *Annu Rev Cell Dev Biol* **23:**175-205.

Chakraborty C, Doss CG, Bandyopadhyay S, and Agoramoorthy G (2014) Influence of miRNA in insulin signaling pathway and insulin resistance: micro-molecules with a major role in type-2 diabetes. *Wiley Interdiscip Rev* RNA **5:**697-712.

Chen AY and Liu LF (1994) Mechanisms of resistance to topoisomerase inhibitors. *Cancer Treat Res* **73:**263-281.

Chen SH, Chan NL, and Hsieh TS (2013) New mechanistic and functional insights into DNA topoisomerases. *Annu Rev Biochem* **82:**139-170.

Corrà F, Agnoletto C, Minotti L, Baldassari F, and Volinia S. (2018) The Network of Non-coding RNAs in Cancer Drug Resistance. *Front Oncol* **8:**327

Cree IA and Charlton P (2017) Molecular chess? Hallmarks of anti-cancer drug resistance. *BMC Cancer* **17:**10.

Deweese JE and Osheroff N (2009) The DNA cleavage reaction of topoisomerase II: wolf in sheep's clothing. *Nucleic Acids Res* **37:**738-748.

Eichhorn SW, Guo H, McGeary SE, Rodriguez-Mias RA, Shin C, Baek D, Hsu SH, Ghoshal K, Villén J, and Bartel DP (2014) mRNA destabilization is the dominant effect of mammalian microRNAs by the time substantial repression ensues. *Mol Cell* **56:**104-115.

Elton TS and Yalowich JC. (2015) Experimental procedures to identify and validate specific mRNA targets of miRNAs. *EXCLI J* **14:**758-790.

Fabian MR and Sonenberg N (2012) The mechanics of miRNA-mediated gene silencing: a look under the hood of miRISC. *Nat Struct Mol Biol* **19:**586-593.

Frankel D, Delecourt V, Harhouri K, De Sandre-Giovannoli A, Lévy N, Kaspi E, and Roll P (2018) MicroRNAs in hereditary and sporadic premature aging syndromes and other laminopathies. *Aging Cell* **17:**e12766.

Fu L, Shi J, Liu A, Zhou L, Jiang M, Fu H, Xu K, Li D, Deng A, Zhang Q, Pang Y, Guo Y, Hu K, Zhou J, Wang Y, Huang W, Jing Y, Dou L, Wang L, Xu K, Ke X, Nervi C, Li Y, and Yu L (2017) A minicircuitry of microRNA-9-1 and RUNX1-RUNX1T1 contributes to leukemogenesis in t(8;21) acute myeloid leukemia. *Int J Cancer* **140:**653-661.

Gabra MM and Salmena L (2017) microRNAs and Acute Myeloid Leukemia Chemoresistance: A Mechanistic Overview. Front Oncol 7:255.

Ganapathi RN and Ganapathi MK (2013) Mechanisms regulating resistance to inhibitors of topoisomerase II. *Front Pharmacol* **4:**89.

Ganger MT, Dietz GD, and Ewing SJ (2017) A common base method for analysis of qPCR data and the application of simple blocking in qPCR experiments. *BMC Bioinformatics* **18:**534.

Griffiths-Jones S (2004) The microRNA Registry. *Nucleic Acids Res* **32:**D109-D111.

Guo H, Ingolia NT, Weissman JS, and Bartel DP (2010) Mammalian microRNAs predominantly act to decrease target mRNA levels. *Nature* **466:**835-840.

Gyori BM, Venkatachalam G, Thiagarajan PS, Hsu D, and Clement MV (2014) OpenComet: an automated tool for comet assay image analysis. *Redox Biol* **2:**457-465.

Ha M and Kim VN (2014) Regulation of microRNA biogenesis. *Nat Rev Mol Cell Biol* **15:**509-524.

Harker, WG, Slade, DL, Parr, RL, and Holguin, MH (1995) Selective use of an alternative stop codon and polyadenylation signal within intron sequences leads to a truncated topoisomerase II alpha messenger RNA and protein in human HL-60 leukemia cells selected for resistance to mitoxantrone. *Cancer Res* **55:**4962–4971.

Hinds M, Deisseroth K, Mayes J, Altschuler E, Jansen R, Ledley FD, and Zwelling LA (1991) Identification of a point mutation in the topoisomerase II gene from a human leukemia cell line containing an amsacrine-resistant form of topoisomerase II. *Cancer Res* **51:**4729-4731.

Hua W, Sa KD, Zhang X, Jia LT, Zhao J, Yang AG, Zhang R, Fan J, and Bian K (2015) MicroRNA-139 suppresses proliferation in luminal type breast cancer cells by targeting Topoisomerase II alpha. *Biochem Biophys Res Commun* **463:**1077-1083.

Jonas S and Izaurralde E (2015) Towards a molecular understanding of microRNA-mediated gene silencing. *Nat Rev Genet* **16:**421-433.

Juźwik CA, Drake SS, Zhang Y, Paradis-Isler N, Sylvester A, Amar-Zifkin A, Douglas C, Morquette B, Moore CS, and Fournier A (2019) microRNA dysregulation in neurodegenerative diseases: A systematic review. *Prog Neurobiol* Jul 26:101664 [Epub ahead of print]

Kanagasabai R, Karmahapatra S, Kientz CA, Yu Y, Hernandez VA, Kania EE, Yalowich JC, and Elton TS (2018) The Novel C-terminal Truncated 90-kDa Isoform of Topoisomerase IIalpha (TOP2alpha/90) Is a Determinant of Etoposide Resistance in K562 Leukemia Cells via Heterodimerization with the TOP2alpha/170 Isoform. *Mol Pharmacol* **93:**515-525.

Kanagasabai R, Serdar L, Karmahapatra S, Kientz CA, Ellis J, Ritke MK, Elton TS, and Yalowich JC (2017) Alternative RNA Processing of Topoisomerase IIalpha in Etoposide-Resistant Human Leukemia K562 Cells: Intron Retention Results in a Novel C-Terminal Truncated 90-kDa Isoform. *J Pharmacol Exp Ther* **360:**152-163.

Khan AA, Betel D, Miller ML, Sander C, Leslie CS, and Marks DS (2009) Transfection of small RNAs globally perturbs gene regulation by endogenous microRNAs. *Nat Biotechnol* **27:**549-555.

Khvorova A, Reynolds A, and Jayasena SD (2003) Functional siRNAs and mi-RNAs exhibit strand bias. *Cell* **115:**209-216.

Kubo A, Yoshikawa A, Hirashima T, Masuda N, Takada M, Takahara J, Fukuoka M, and Nakagawa K (1996) Point mutation of the topoisomerase IIα gene in pateins with small cell cancer treated with etoposide. *Cancer Res* **56:**1232-1236.

Kuchenbauer F, Mah SM, Heuser M, McPherson A, Ruschmann J, Rouhi A, Berg T, Bullinger L, Argiropoulos B, Morin RD, Lai D, Starczynowski DT, Karsan A, Eaves CJ, Watahiki A, Wang Y, Aparicio SA, Ganser A, Krauter J, Döhner H, Döhner K, Marra MA, Camargo FD, Palmqvist L, Buske C, and Humphries RK (2011) Comprehensive analysis of mammalian miRNA* species and their role in myeloid cells. *Blood* **118:**3350-3358.

Kuhn DE, Martin MM, Feldman DS, Terry AV Jr, Nuovo GJ, and Elton TS. (2008) experimental validation of miRNA targets. *Methods* **44:**47-54.

Kunej T, Godnic I, Ferdin J, Horvat S, Dovc P, and Calin GA (2011) Epigenetic regulation of microRNAs in cancer: an integrated review of literature. *Mutat Res* **717:**77-84.

Langmead B, Trapnell C, Pop M, and Salzberg SL (2009) Ultrafast and memory-efficient alignment of short DNA sequences to the human genome. *Genome Biol* **10:**R25.

Laponogov I, Pan XS, Veselkov DA, McAuley KE, Fisher LM, and Sanderson MR (2010) Structural basis of gate-DNA breakage and resealing by type II topoisomerases. *PLoS One* **5:**e11338.

Larsen AK, Escargueil AE, and Skladanowski A (2003) Catalytic topoisomerase II inhibitors in cancer therapy. *Pharmacol Ther* **99:**167-181.

Li H, Handsaker B, Wysoker A, Fennell T, Ruan J, Homer N, Marth G, Abecasis G, Durbin R; 1000 Genome Project Data Processing Subgroup (2009) The Sequence Alignment/Map format and SAMtools. *Bioinformatics* **25:**2078-2079.

Li X, Pan Q, Wan X, Mao Y, Lu W, Xie X, and Cheng X (2015) Methylation-associated Hsa-miR-9 deregulation in paclitaxel resistant epithelial ovarian carcinoma. *BMC Cancer* **15:**509.

Li Y, Zhao L, Li N, Miao Y, Zhou H, and Jia L (2017) miR-9 regulates the multidrug resistance of chronic myelogenous leukemia by targeting ABCB1. *Oncol Rep* **37:**2193-2200.

Liao Y, Smyth GK, and Shi W (2014) featureCounts: an efficient general purpose program for assigning sequence reads to genomic features. *Bioinformatics* **30:**923-930.

Liu Y, Lei P, Qiao H, Sun K, Lu X, Bao F, Yu R, Lian C, Li Y, Chen W, and Xue F (2019) miR-9 Enhances the Chemosensitivity of AML Cells to Daunorubicin by Targeting the EIF5A2/MCL-1 Axis. *Int J Biol Sci* **15:**579-586.

Martin M (2011) Cutadapt removes adapter sequences from high-throughput sequencing reads. *EMBnet.journal* **17:**10-12.

Mirski, SE and Cole, SP. (1995) Cytoplasmic localization of a mutant M(r) 160,000 topoisomerase II alpha is associated with the loss of putative bipartite nuclear localization signals in a drug-resistant human lung cancer cell line. *Cancer Res* **55:**2129–2134.

Mirski SE, Evans CD, Almquist KC, Slovak ML, and Cole SP. (1993) Altered topoisomerase II alpha in a drug-resistant small cell lung cancer cell line selected in VP-16. *Cancer Re*s **53**:4866-4873.

Mirski, SE, Sparks, KE, Yu, Q, Lang, AJ, Jain, N, Campling, BG, and Cole, SP. (2000) A truncated cytoplasmic topoisomerase II alpha in a drug-resistant lung cancer cell line is encoded by a TOP2A allele with a partial deletion of exon 34. *Int J Cancer* **85:**534-539.

Munoz JL, Bliss SA, Greco SJ, Ramkissoon SH, Ligon KL, and Rameshwar P (2013) Delivery of Functional Anti-miR-9 by Mesenchymal Stem Cell-derived Exosomes to Glioblastoma Multiforme Cells Conferred Chemosensitivity. *Mol Ther Nucleic Acids* **2:**e126.

Munoz JL, Rodriguez-Cruz V, and Rameshwar P (2015) High expression of miR-9 in CD133^{+} glioblastoma cells in chemoresistance to temozolomide. *J Cancer Stem Cell Res* **3:**e1003.

Munoz JL, Rodriguez-Cruz V, Ramkissoon SH, Ligon KL, Greco SJ, and Rameshwar P (2015) Temozolomide resistance in glioblastoma occurs by miRNA-9-targeted PTCH1, independent of sonic hedgehog level. *Oncotarget* **6:**1190-1201.

Nass D, Rosenwald S, Meiri E, Gilad S, Tabibian-Keissar H, Schlosberg A, Kuker H, Sion-Vardy N, Tobar A, Kharenko O, Sitbon E, Lithwick Yanai G, Elyakim E, Cholakh H, Gibori H, Spector Y, Bentwich Z, Barshack I, and Rosenfeld N (2009) MiR-92b and miR-9/9* are specifically expressed in brain primary tumors and can be used to differentiate primary from metastatic brain tumors. *Brain Pathol* **19:**375-383.

Nitiss JL (2009) Targeting DNA topoisomerase II in cancer chemotherapy. *Nat Rev Cancer* **9:**338-350.

Nowek K, Sun SM, Bullinger L, Bindels EM, Exalto C, Dijkstra MK, van Lom K, Döhner H, Erkeland SJ, Löwenberg B, and Jongen-Lavrencic M (2016) Aberrant expression of miR-9/9* in myeloid progenitors inhibits neutrophil differentiation by post-transcriptional regulation of ERG. *Leukemia* **30:**229-37.

Nowek K, Wiemer EAC, and Jongen-Lavrencic M (2018) The versatile nature of miR-9/9(*) in human cancer. *Oncotarget* **9:**20838-20854.

Nugent M (2016) MicroRNAs: exploring new horizons in osteoarthritis. *Osteoarthritis Cartilage* **24:**573-580.

Olive PL (2002) The comet assay. An overview of techniques. *Methods Mol Biol* **203:**179-194.

Packer AN, Xing Y, Harper SQ, Jones L, and Davidson BL (2008) The bifunctional microRNA miR-9/miR-9* regulates REST and CoREST and is downregulated in Huntington's disease. *J Neurosci* **28:**14341-14346.

Paraskevopoulou MD, Georgakilas G, Kostoulas N, Vlachos IS, Vergoulis T, Reczko M, Filippidis C, Dalamagas T, and Hatzigeorgiou AG (2013) DIANA-microT web server v5.0: service integration into miRNA functional analysis workflows. *Nucleic Acids Res* **41:**169.

Pendleton M, Lindsey RH,Jr, Felix CA, Grimwade D, and Osheroff N (2014) Topoisomerase II and leukemia. *Ann N Y Acad Sci* **1310:**98-110.

Pilati P, Nitti D, and Mocellin S (2012) Cancer resistance to type II topoisomerase inhibitors. *Curr Med Chem* **19:**3900-3906.

Pommier Y, Leo E, Zhang H, and Marchand C (2010) DNA topoisomerases and their poisoning by anticancer and antibacterial drugs. *Chem Biol* **17:**421-433.

Raghuwanshi S, Gutti U, Kandi R, and Gutti RK (2018) MicroRNA-9 promotes cell proliferation by regulating RUNX1 expression in human megakaryocyte development. *Cell Prolif* **51:**e12414.

Ritchie, ME, Phipson, B, Wu, D, Hu, Y, Law, CW, Shi, W, and Smyth, GK (2015) limma powers differential expression analyses for RNA-sequencing and microarray studies. *Nucleic Acids Research* **43:**e47.

Ritke MK and Yalowich JC (1993) Altered gene expression in human leukemia K562 cells selected for resistance to etoposide. *Biochem Pharmacol* **46:**2007-2020.

Ritke, MK, Roberts, D, Allan, WP, Raymond, J, Bergoltz, VV, and Yalowich, JC. (1994) Altered stability of etoposide-induced topoisomerase Il-DNA complexes in resistant human leukemia K562 cells. *Br J Cancer* **69:**687-697.

Ro S, Park C, Young D, Sanders KM, and Yan W (2007) Tissue-dependent paired expression of miRNAs. *Nucleic Acids Res* **35:**5944-5953.

Roese-Koerner B, Stappert L, Berger T, Braun NC, Veltel M, Jungverdorben J, Evert BO, Peitz M, Borghese L, and Brüstle O (2016) Reciprocal Regulation between Bifunctional miR-9/9(*) and its Transcriptional Modulator Notch in Human Neural Stem Cell Self-Renewal and Differentiation. *Stem Cell Reports* **7:**207-219.

Sansom SE, Nuovo GJ, Martin MM, Kotha SR, Parinandi NL, and Elton TS. (2010) miR-802 regulates human angiotensin II type 1 receptor expression in intestinal epithelial C2BBe1 cells. *Am J Physiol Gastrointest Liver Physiol* **299:**G632-642.

Schmittgen TD and Livak KJ (2008) Analyzing real-time PCR data by the comparative C(T) method. Nat Protoc 3:1101-1108.

Schraivogel D, Weinmann L, Beier D, Tabatabai G, Eichner A, Zhu JY, Anton M, Sixt M, Weller M, Beier CP, and Meister G (2011) CAMTA1 is a novel tumour suppressor regulated by miR-9/9* in glioblastoma stem cells. *EMBO J* **30:**4309-4322.

Schwarz DS, Hutvágner G, Du T, Xu Z, Aronin N, and Zamore PD (2003) Asymmetry in the assembly of the RNAi enzyme complex. *Cell* **115:**199-208.

Sun C, Li N, Yang Z, Zhou B, He Y, Weng D, Fang Y, Wu P, Chen P, Yang X, Ma D, Zhou J, and Chen G (2013) miR-9 regulation of BRCA1 and ovarian Cancer sensitivity to cisplatin and PARP inhibition. *J Natl Cancer Inst* **105:**1750-1758.

Suzuki H, Maruyama R, Yamamoto E, and Kai M (2013) Epigenetic alteration and microRNA dysregulation in cancer. *Front Genet* **4:**258.

Tian J, Rui K, Tang X, Ma J, Wang Y, Tian X, Zhang Y, Xu H, Lu L, and Wang S (2015) MicroRNA-9 Regulates the Differentiation and Function of Myeloid-Derived Suppressor Cells via Targeting Runx1. *J Immunol* **195:**1301-1311.

Treiber T, Treiber N, and Meister G (2019) Regulation of microRNA biogenesis and its crosstalk with other cellular pathways. *Nat Rev Mol Cell Biol* **20:**5-20.

Vassetzky YS, Alghisi GC, and Gasser SM (1995) DNA topoisomerase II mutations and resistance to anti-tumor drugs. *BioEssays* **17:**767-774.

Vlasova II, Feng WH, Goff JP, Giorgianni A, Do D, Gollin SM, Lewis DW, Kagan VE, and Yalowich JC (2011) Myeloperoxidase-dependent oxidation of etoposide in human myeloid progenitor CD34+ cells. *Mol Pharmacol* **79:**479-487.

Vos SM, Tretter EM, Schmidt BH, and Berger JM (2011) All tangled up: how cells direct, manage and exploit topoisomerase function. *Nat Rev Mol Cell Biol* **12:**827-841.

Wessel I, Jensen PB, Falck J, Mirski SE, Cole SP, and Sehested M (1997) Loss of amino acids 1490Lys-Ser-Lys1492 in the COOH-terminal region of topoisomerase II alpha in human small cell lung cancer cells selected for resistance to etoposide results in an extranuclear enzyme localization. *Cancer Res* **57:**4451-4454.

Yuva-Aydemir Y, Simkin A, Gascon E, and Gao FB (2011) MicroRNA-9: functional evolution of a conserved small regulatory RNA. *RNA Biol* **8:**557-564.

Yu Q, Mirski S, Sparks KE, and Cole, SP (1997) Two COOH-terminal truncated cytoplasmic forms of topoisomerase II alpha in a VP-16-selected lung cancer cell line result from partial gene deletion and alternative splicing. *Biochemistry* **36:**5868-5877.

Zahreddine H and Borden KL (2013) Mechanisms and insights into drug resistance in cancer. *Front Pharmacol* **4:**28.

Zwelling LA, Hinds M, Chan D, Mayes J, Sie KL, Parker E, Silberman L, Radcliffe A, Beran M, and Blick M (1989) Characterization of an amsacrine-resistant line of human leukemia cells. Evidence for a drug-resistant form of topoisomerase II. *J Biol Chem* **264:**16411-16420.

Footnotes

Acknowledgements

40

Figure Legends

Fig 1. K/VP.5 cell resistance to etoposide is associated with attenuated TOP2α/170 mRNA and protein levels. (A) Parental K562 and K/VP.5 cells with acquired resistance to etoposide were incubated with increasing concentrations of etoposide for 48 hr, and the cells were then counted. The extent of growth (beyond initial concentration of 1 x 10^5 cell/ml) in drug-treated versus control was ultimately expressed as percent inhibition of control growth. Results are shown as a scattergram from 4 independent experiments performed on separate days. (B) qPCR experiments were performed utilizing K562 and K/VP.5 cDNAs and a TaqMan hydrolysis assay specific for TOP2α/170. Results shown are the mean ± S.D. from 5 RNA/cDNA isolations/determinations performed on separate days; K/VP.5 versus K562 for expression of TOP2α/170 mRNA ($P < 0.001$). Calculated $2^{-\Delta Ct}$ values from qPCR assays were log transformed to assure distribution normality prior to data analysis using a two-tailed paired Student's t-test. (C) Representative immunoassay using K562 and K/VP.5 cellular lysates. Blots were probed with antibodies specific for the N-terminal portion of TOP2α/170 (i.e., amino acids 14–27) or for GAPDH. Averaging results from 5 separate paired collections of K562 and K/VP.5 cells on different days, there was a reduction of TOP2α/170 in K/VP.5 cells to 10.6% the level found in parental K562 cells taking into account the GAPDH loading control ($P = 0.014$).

Fig 2. miR-9-3p and miR-9-5p are overexpressed in K/VP.5 cells. (A) Volcano plot analysis of miRNAs over- or underexpressed in K/VP.5 compared to K562 cells. Differentially expressed miRNAs are defined as those with at least a ± two-fold change [red circles outside vertical dotted lines and above the horizontal dotted line ($P < 0.05$)]. (B) Schematic representation of the location of putative MREs harbored in the 3′-UTR of TOP2α/170 mRNA. Additionally the "seed sequence" complementarity is shown between miR-9-3p and miR-9-5p and the putative TOP2α/170 3′-UTR MREs. (C) qPCR utilizing K562 and K/VP.5 cDNAs and TaqMan hydrolysis assays specific for

miR-9-3p and miR-9-5p. Results shown are the mean ± S.D. for 3 determinations made from 3 separate RNA/cDNA preparations made on separate days; *$P < 0.001$, comparing K/VP.5 to K562 cell levels of miR-9-3p and miR-9-5p. (D) qPCR utilizing K562 and K/VP.5 cDNAs and TaqMan hydrolysis assays specific for pri-miRNAs (i.e., mir-9-1, mir-9-2, and mir-9-3) transcribed from 3 independent genes; MIR9-1, MIR9-2, and MIR9-3. Results shown are the mean ± S.D. from 4-7 determinations made from separate RNA/cDNA preparations; *$P < 0.001$(N=7); comparing K/VP.5 to K562 cell levels of mir-9-1; *$P = 0.078$ (N=4); comparing K/VP.5 to K562 cell levels of mir-9-3. For Fig. 2C and 2D, calculated $2^{-\Delta Ct}$ values from qPCR assays were log transformed to assure distribution normality prior to data analysis using a two-tailed paired Student's t-test.

Fig 3. miR-9-3p and miR-9-5p directly interact with the TOP2α/170 3′-UTR. (A) K562 and K/VP.5 cells were transfected with the psiTOP2α/170/UTR luciferase reporter construct (1 μg). Forty-eight hr later, luciferase activities were measured. Renilla luciferase activity was normalized to firefly luciferase activity. Results shown are the mean ± S.D. from 17 experiments performed on separate days; *$P < 0.001$, K/VP.5 luciferase versus K562 luciferase levels. (B) K562 cells were cotransfected with the psiTOP2α/170/UTR luciferase reporter construct (1 μg) and either control, miR-9-3p, or miR-9-5p mimics (25 nM). Forty-eight hr later, total RNA was isolated and reverse transcribed. qPCR experiments were performed utilizing K562 cDNAs and TaqMan hydrolysis assays specific for miR-9-3p and miR-9-5p. Results shown are the mean ± S.D. from 5 experiments performed on separate days; *$P < 0.001$, miR-9-3p levels in miR-9-3p mimic transfected K562 versus nontransfected K562 cells, and miR-9-5p levels in miR-9-5p mimic transfected K562 versus nontransfected K562 cells, respectively. mir-9-5p was not significantly increased in mir-9-3p mimic transfected cells ($P = 0.340$) nor was mir-9-3p significantly increased

in mir-9-5p mimic transfected cells ($P = 0.223$). Calculated $2^{-\Delta Ct}$ values from qPCR assays were log transformed to assure distribution normality prior to data analysis using a two-tailed paired Student's t-test. (C) K562 cells were cotransfected with the psiTOP2α/170/UTR luciferase reporter construct (1 µg) and either control, miR-9-3p, or miR-9-5p mimics (25 nM). Forty eight hr later, luciferase activities were measured. Results shown are the mean ± S.D. from 9 experiments performed on separate days; $P < 0.05$ for miR-9-3p mimic and miR-9-5p mimic versus control mimic transfected K562 cells. (D) K562 cells were cotransfected with luciferase constructs, where the miR-9-3p and miR-9-5p putative binding sites were mutated (shown schematically), and either control, miR-9-3p, or miR-9-5p mimics (25 nM). Forty eight hr later, luciferase activities were measured. Results shown are the mean ± S.D. from 3-5 experiments performed on separate days.

Fig 4. miR-9-3p and miR-9-5p overexpression results in decreased TOP2α/170 protein and reduced etoposide-induced DNA damage in K562 cells. (A) Representative immunoassay using cellular lysates from K562 cells that were transfected (48 hr) with control, miR-9-3p, miR-9-5p mimics (25 nM), or transfectant reagent alone (Lipofectamine--mock control). Blots were probed with antibodies specific for the N-terminal portion of TOP2α/170 (i.e., amino acids 14–27) or for GAPDH. (B) Expression of TOP2α/170 protein levels in K562 cells transfected (48 hr) with either control, miR-9-3p, or miR-9-5p mimics (25 nM). Results shown are the mean ± S.D. from 5 experiments performed on separate days; *$P < 0.05$ comparing miR-9-3p and miR-9-5p mimic transfected K562 lysates versus control mimic transfected K562 lysates. (C) Etoposide (2 and 5 µM)-induced DNA damage in control, miR-9-3p, or miR-9-5p mimic (25 nM) transfected (48 hr) K562 cells was determined by Comet assays after a 1-hour incubation and subtraction of DMSO vehicle controls, as described in Materials and Methods. Results shown are the mean ± S.D. from

43

7 experiments performed on separate days; *$P < 0.05$ comparing miR-9-3p and miR-9-5p mimic transfected versus control mimic transfected K562 cells. (D) TOP2α/170 mRNA levels in K562 cells transfected (48 hr) with either control, miR-9-3p, or miR-9-5p mimics (25 nM). Results shown are the mean ± S.D. from 3 experiments performed on separate days.

Fig 5. miR-9-3p and miR-9-5p inhibitors increase TOP2α/170 protein and enhance etoposide-induced DNA damage in K/VP.5 cells. (A) Representative immunoassay using cellular lysates from K/VP.5 cells that were transfected (48 hr) with either control, miR-9-3p, or miR-9-5p inhibitors (25 nM). Blots were probed with an antibodies specific for the N-terminal portion of TOP2α/170 (i.e., amino acids 14–27) or for GAPDH. (B) Expression of TOP2α/170 protein levels in K/VP.5 cells transfected (48 hr) with either control, miR-9-3p, or miR-9-5p inhibitors (25 nM). Results shown are the mean ± S.D. from 5 experiments performed on separate days; *$P < 0.05$ comparing miR-9-3p and miR-9-5p inhibitor transfected K/VP.5 lysates versus control inhibitor transfected K/VP.5 lysates. (C) Etoposide (10 and 25 μM)-induced DNA damage in control, miR-9-3p, or miR-9-5p inhibitor (25 nM) transfected K/VP.5 cells (48 hr) was determined by Comet assays after a 1-hr incubation and subtraction of DMSO vehicle controls, as described in Materials and Methods. Results shown are the mean ± S.D. from 6 experiments performed on separate days; *$P < 0.05$ comparing miR-9-3p and miR-9-5p inhibitor transfected versus control inhibitor transfected K/VP.5 cells. (D) Expression of TOP2α/170 mRNA levels in K/VP.5 cells transfected (48 hr) with either control, miR-9-3p, or miR-9-5p inhibitors (25 nM). Results shown are the mean ± S.D. from 5 experiments performed on separate days.
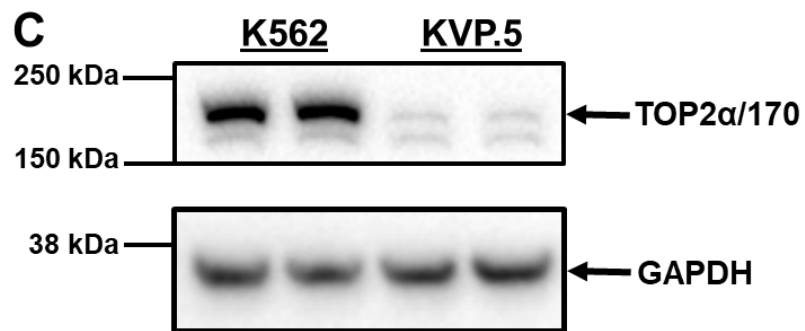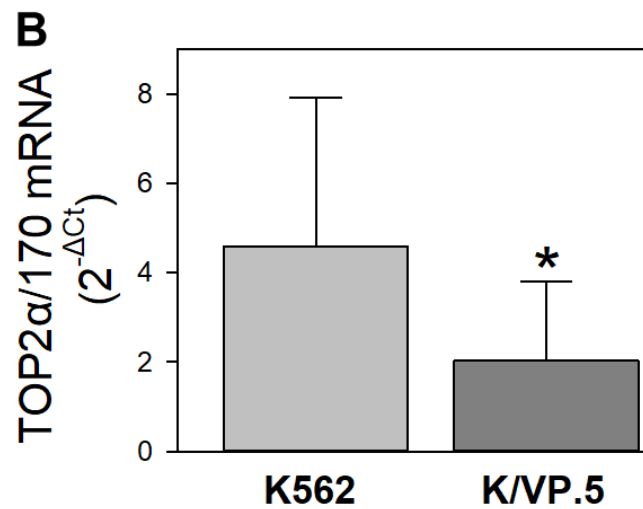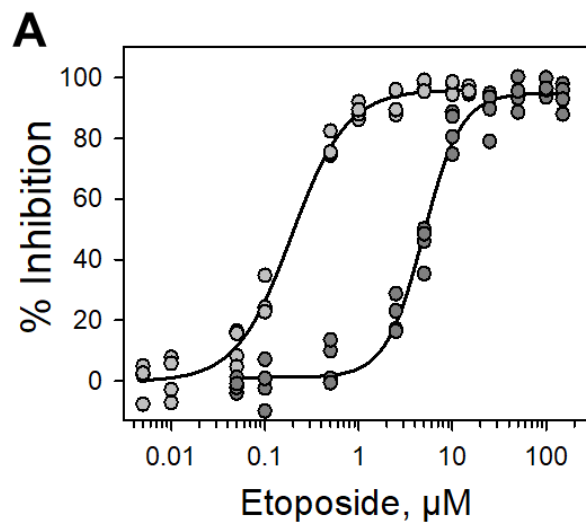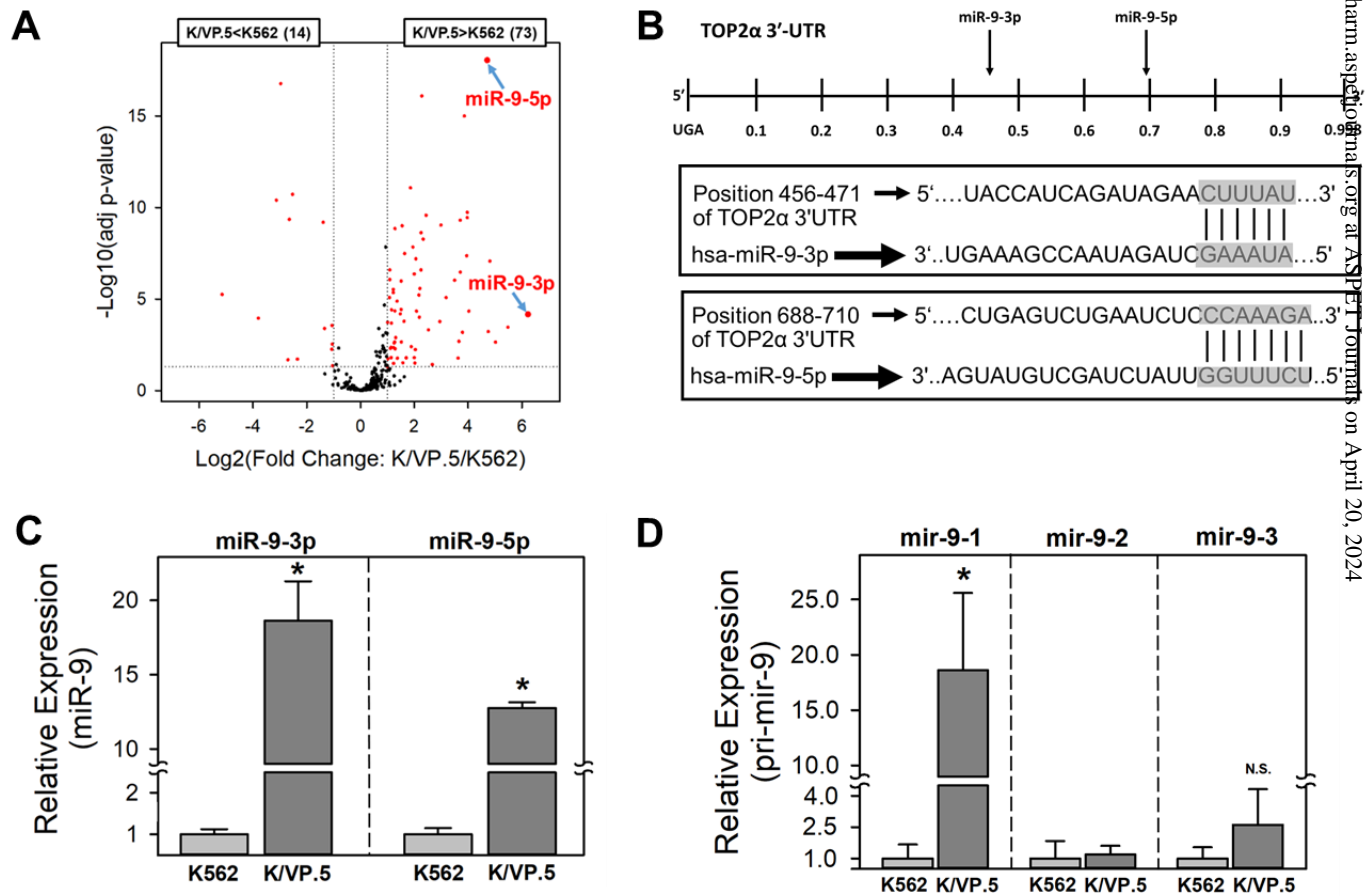
Figure 1

Figure 2

Figure 3

Figure 4

Figure 5